INTERA Incorporated
9600 Great Hills Trail, Suite 300W
Austin, Texas 78759 USA
512.425.2000

June 13, 2026

Aaron K. Schindewolf, P.E.
Project Manager 2
San Jacinto River Authority
2436 Sawdust Road
The Woodlands, TX 77380

RE: Review of Twentieth (20th) Re-measure of Elevations at Monitoring Benchmarks and Monitoring Points Along the Water Line Segments W1A and W2A in the Woodlands, Texas

Dear Aaron:

This letter provides INTERA's review of the March 2026 re-measure of elevations for monitoring benchmarks and monitoring points along the water line Segments W1A and W2A in The Woodlands, Texas. This review is provided in Attachment A. Attachment A also includes a review of the water line tolerances along Segments W1A and W2A compared to land subsidence.

The work was performed under Purchase Order PO002296. The technical lead for this work is Dr. Steven Young.

Respectfully submitted,

Steven C Young

Steven Young, PHD
Professional Geologist
INTERA Incorporated

Enclosure

ATTACHMENT A

Review of Twentieth (20) Re-measure of the Elevations at Monitoring Points and Monitoring Benchmarks along Water Line Segments W1A and W2A

Geoscientist Seal

Dr. Steven C. Young, performed or supervised all services associated with preparing Attachment A. The geoscientific services included the writing the text, data analysis, tabulation of results, and construction of figures. I am employed by INTERA Incorporated in Austin, Texas. INTERA is Professional Geoscience firm, with registration number 50189. Dr. Young professional geoscience registration number is 231.

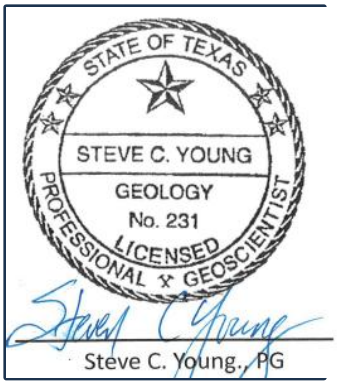

Overview of Twentieth (20th) Re-measure of the Elevations at Monitoring Points and Monitoring Benchmarks along Water Line Segments W1A and W2A

In March 2015, an SJRA contracted surveyor began measuring elevations of monitoring points and monitoring benchmarks along the water line segments W1A and W2A. Since March 2015, the SJRA contracted surveyor has re-measured the elevations of the monitoring points and monitoring benchmarks along the water line segments W1A and W2A. In March 2026, the SJRA contracted surveyor performed the Twentieth re-measurement.

Figure 1 shows the locations of the water line segments W1A and W2A and the four monitoring systems. Each of the monitoring systems consists of monitoring points or monitoring benchmarks. Monitoring benchmarks terminate in the ground and are used to measure elevation changes in the soil. Monitoring points terminate on top of a pipe or a pipe casing and are used to measure the elevation changes of the water line. The Egypt Fault Monitoring System and the Big Barn Fault Monitoring System consists only of monitoring points. The Segment W1A Monitoring System and Segment W2A Monitoring System consist of only monitoring benchmarks.

Figure 2 is a satellite map that shows the San Jacinto River Authority (SJRA) Groundwater Reduction Plan (GRP) water line and the faults that have been identified in the vicinity of water line segments W1A and W2A by Fugro (2012). The lateral extent of the Egypt, Big Barn, Jones, and suspected Panther Branch faults reported by Fugro (2012) are represented by the georeferenced fault lines. In their study, Fugro (2012) did not extend the Panther Branch Fault across the SJRA GRP water line route. INTERA mapped the interpolated portion of the suspected Panther Branch Fault in Figure 2 in 2021 based on an evaluation of the monitoring benchmark elevation for Segment W2A and aerial photographs of scarp locations in the parking lot of The Woodlands High School.

The March 2026 survey represents the Twentieth (20th) re-measure of the elevations since their initial measurements in March 2015. Re-measurements were made about every six months until March 2024. After March 2024, re-measurements are currently planned for every 12 months for the next several years. **Table 1** shows the re-measured elevations for the monitoring benchmarks located near the Egypt Fault that comprise Segment W1A Monitoring System. **Table 2** shows the re-measured elevations for the monitoring points that comprise the Egypt Fault Monitoring System. **Table 3** shows the re-measured

elevations for the monitoring points that comprise the Big Barn Fault Monitoring System. **Table 4** shows the re-measured elevations for the monitoring benchmarks located near the suspected Panther Branch Fault that comprise the Segment W2A Monitoring System.

Table 1 Elevations for the Egypt Fault Monitoring Benchmarks along SJRA Segment W1A Monitoring Survey for March 2015, March 2025, and March 2026

Point ID	Measured Elevation			Calculated Differences	
	(a) Initial Survey March 2015 Elev. (ft msl)	(b) March 2025 Elev. (ft msl)	(c) March 2026 Elev. (ft msl)	March 2026 minus March 2015 (c) - (a)	March 2026 minus March 2025 (c) - (b)
MbM-1	189.24	189.25	189.25	0.01	0.00
MbM-2	189.27	189.28	189.27	0.00	-0.01
MbM-3	189.45	189.43	189.43	-0.02	0.00
MbM-4	189.73	189.73	189.72	-0.01	-0.01
MbM-5	190.41	Destroyed	Destroyed	na	na
MbM-6	190.26	Destroyed	Destroyed	na	na
MbM-7	188.81	188.82	188.80	-0.01	-0.02
MbM-8	188.28	188.29	188.27	-0.01	-0.02
MbM-9	187.93	187.93	187.92	-0.01	-0.01
MbM-10	187.76	187.76	187.75	-0.01	-0.01
MbM-11	188.00	187.80	187.78	-0.22	-0.02
MbM-12	187.77	187.76	187.75	-0.02	-0.01
MbM-13	187.50	187.50	187.48	-0.02	-0.02
MbM-14	187.75	187.74	187.73	-0.02	-0.01
MbM-15	188.49	188.49	188.47	-0.02	-0.02
MbM-16	187.86	187.85	187.83	-0.03	-0.02
MbM-17	189.31	189.30	189.29	-0.02	-0.01
MbM-18	189.75	189.74	189.72	-0.03	-0.02
MbM-19	189.32	189.31	189.29	-0.03	-0.02
MbM-20	188.55	188.53	188.52	-0.03	-0.01

note: na= not applicable

Table 2 Elevations for Monitoring Points Along SJRA Segment W1A for March 2015, March 2025, and March 2026 at Existing Fault Protection System Egypt Fault

Station/Description	Measured Elevation			Calculated Differences	
	(a) Initial Survey March 2015 Elev. (ft msl)	(b) March 2025 Elev. (ft msl)	(c) March 2026 Elev. (ft msl)	March 2026 minus March 2015 (c) - (a)	March 2026 minus March 2025 (c) - (b)
Sta 103 + 72 Top Square Nut on 2" Steel Cap	187.20	187.19	187.19	-0.01	0.00
Sta 103 + 82 Top 2" Steel Pipe (NO CAP)	186.93	186.92	186.91	-0.02	-0.01
Sta 108 + 70 Top Square Nut on 2" Steel Cap	190.28	190.22	190.21	-0.07	-0.01
Sta 108 + 80 Top 2" Steel Cap	190.31	190.26	190.25	-0.06	-0.01

Table 3 Elevations for Monitoring Points along SJRA Segment W2A for March 2015, March 2025, and March 2026 at Existing Fault Protection System Big Barn Fault

Station/Description	Measured Elevation			Calculated Differences	
	(a) Initial Survey March 2015 Elev. (ft, msl)	(b) March 2025 Elev. (ft msl)	(c) March 2026 Elev. (ft msl)	March 2026 minus March 2015 (c) - (a)	March 2026 minus March 2025 (c) - (b)
Sta 9 + 25 Top 2" Steel Cap	177.81	177.81	177.82	0.01	0.01
Sta 9 + 35 Top 2" Steel Cap	177.74	177.74	177.74	0.00	0.00
Sta 9 + 85 Top 2" Steel Cap	176.73	176.70	176.70	-0.03	0.00
Sta 9 + 95 Top 2" Steel Cap	176.78	176.75	176.75	-0.03	0.00

Table 4 Elevations for Monitoring Benchmarks that Straddle the Suspected Panther Branch Fault along SJRA Segment W2A Monitoring Survey for March 2015, March 2025, and March 2026

Point ID	Measured Elevation			Calculated Differences	
	(a) Initial Survey March 2015 Elev. (ft, msl)	(b) March 2025 Elev. (ft msl)	(c) March 2026 Elev. (ft msl)	March 2026 minus March 2015 (c) - (a)	March 2026 minus March 2025 (c) - (b)
MbM-1	142.59	142.48	142.47	-0.12	-0.01
MbM-2	142.80	142.68	142.67	-0.13	-0.01
MbM-3	143.31	143.18	143.16	-0.15	-0.02
MbM-4	143.35	143.20	143.18	-0.17	-0.02
MbM-5	143.85	143.73	143.71	-0.14	-0.02
MbM-6	144.14	144.04	144.02	-0.12	-0.02
MbM-7	144.29	144.19	144.18	-0.11	-0.01
MbM-8	145.20	145.09	145.07	-0.13	-0.02
MbM-9	145.51	145.41	145.39	-0.12	-0.02
MbM-10	145.63	145.52	145.50	-0.13	-0.02
MbM-11	146.16	146.11	146.10	-0.06	-0.01
MbM-12	145.42	145.37	145.36	-0.06	-0.01
MbM-13	145.00	145.00	144.99	-0.01	-0.01
MbM-14	144.99	144.98	144.98	-0.01	0.00
MbM-15	144.79	144.79	144.79	0.00	0.00
MbM-16	144.78	144.78	144.78	0.00	0.00
MbM-17	144.79	144.79	144.78	-0.01	-0.01
MbM-18	144.55	144.54	144.54	-0.01	0.00
MbM-20	145.86	145.75	145.74	-0.12	-0.01

At the Egypt Fault Monitoring System (see **Figures 2** and **3**) and the Big Barn Fault Monitoring System (see **Figures 2** and **4**), SJRA hired consultants to design and contractors to build safeguards to protect the water line from potential damage caused by fault movement. At these two locations, SJRA also hired a consultant to install monitoring points to monitor changes in the elevation of the transmission pipe and casing near the faults. At the water line segment W1A Monitoring System (Figures 2 and 3), SJRA hired a consultant to design and a contractor to build safeguards to protect the water line from potential damage caused by fault movement. Additionally, at the water line segment W1A Monitoring System, SJRA hired consultants to install monitoring benchmarks to monitor changes in land elevations over time.

At the water line segment W2A Monitoring System (see **Figure 5**) along Research Forest Drive no safeguards similar to those installed for the Big Barn Fault and the Egypt Fault were constructed to protect the water line from possible damage caused by fault movement because the Fugro report (2012) did not

show the suspected Panther Branch Fault crossing the water line. However, SJRA hired consultants to install monitoring benchmarks capable of monitoring the change in land elevation at the Segment W2A Monitoring System (see Figure 5) along Research Forest Drive in the vicinity of the suspected Panther Branch Fault.

The labeling of the downthrown and the upthrown side of the faults in Figures 3, 4, and 5 is based on the information presented by Fugro (2012) in their Plate 1. The designations of the two sides of a fault are based on the historical vertical movement of the fault. The downthrown side of the fault has historically moved downward relative to the upthrown side of the fault.

Egypt Fault Monitoring System – At the Egypt Fault Monitoring System (Figure 3), the changes in the elevations from March 2015 to March 2026 indicate that a greater decrease in pipe/casing elevation occurred on the downthrown side than on the upthrown side of the Egypt Fault. Over a 11-year period from 2015 to 2026, the pipe/casing elevation on the downthrown side of the Egypt Fault decreased 0.05 ft relative to the upthrown side of the Egypt Fault. The 0.05 ft decrease over an 11-year period translates into an average subsidence rate of approximately 0.0045 ft/yr.

W1A Segment – At the W1A segment where 18 monitoring benchmarks are located along FM 2978 (Figure 3), the changes in monitoring benchmark elevations from March 2015 to March 2026 indicate that a greater decrease in land elevation has occurred on the downthrown side than on the upthrown side of the Egypt Fault. Over the 11-year period from 2015 to 2026, the land surface on downthrown side of the Egypt Fault decreased 0.015 ft in elevation relative to the upthrown side of the Egypt Fault. The 0.015 ft decrease in land elevation over an 11-year period translates into an average subsidence rate of approximately 0.0014 ft/yr (note: as explained below benchmark 11 was not included in the analysis).

Big Barn Monitoring System – At the Big Barn Fault Monitoring System where four monitoring points on Research Forest Drive straddle the Big Barn Fault (Figure 4), the changes in the monitoring benchmark elevations indicate that a greater decrease in pipe/casing elevation has occurred on the downthrown side than on the upthrown side of the Big Barn Fault. Based on the change in elevations of the four monitoring benchmarks over an 11-year period from March 2015 to March 2026, the pipe/casing elevation on downthrown side of the Big Barn Fault decreased 0.035 ft relative to the upthrown side of the Big Barn Fault. The 0.035 ft decrease in pipe/casing over an 11-year period translates into average subsidence rate of approximately 0.0032 ft/yr.

W2A Segment – Along the W2A segment where 19 monitoring benchmarks on Research Forest Drive are located near the suspected Panther Branch Fault (Figure 5), the changes in the monitoring benchmark elevations suggest that greater land subsidence has occurred on the downthrown side than on the upthrown side of the suspected Panther Branch Fault. Based on the change in elevations of the 19 monitoring benchmarks over an 11-year period from March 2015 to March 2026, the land surface on downthrown side of the suspected Panther Branch Fault decreased 0.113 ft in elevation relative to the upthrown side of the suspected Panther Branch Fault. The 0.113 ft decrease in land elevation over an 11-year period translates into an average subsidence rate of approximately 0.0103 feet per year (ft /yr).

Based on the changes in monitoring benchmark elevations and benchmark points during the last 11 years, the SJRA GRP water line is not at risk of damage from land subsidence where it crosses the Egypt Fault and the Big Barn Fault for the next 50 years if land subsidence continues at its current rate and if the consultant's safeguards work as designed. For the suspected Panther Branch Fault, the amount of subsidence that has occurred since March 2015 does not pose a threat to the safety of water line based on INTERA's discussion with SJRA consultants who designed the water line. However, INTERA recommends SJRA continue with studies of the suspected Panther Branch Fault study to determine if and

where the suspected Panther Branch Fault crosses the SJRA GRP water line and whether mitigation measures will be needed in future.

General Comment on Interpretating the Re-Measured Monitoring Points and Monitoring Benchmark Elevations for Evidence of Land Subsidence

Given that the measured elevations are reported to the nearest hundredth of a foot, an actual elevation difference of just one one-thousandth (0.001) of a foot (from 0.004 to 0.005) could result in a change in reported elevation of one one-hundredth (0.01) of a foot because of the impact of rounding from thousandths to hundredths of a foot. Thus, elevation changes of a few hundredths of a foot and less should be viewed with care before making conclusions regarding the changes in land elevations inferred from the measured elevations. In addition, other mechanisms besides depressurization of the regional aquifer should be evaluated as possible contributors for changes in land elevation before making conclusions regarding the cause for subsidence and predictions of future subsidence. Another mechanism is shrinkage of clayey soils.

Expansive clay soils like vertisols are relatively common in Harris County. These soils absorb water like a sponge and swell during wet periods and dry out and shrink during dry periods. Shrinkage of clay soils causes subsidence but unlike subsidence caused by pumping, the consolidation of the soil is confined to shallow depths. As a result, shrinkage of clay soil that occurs near ground surface will have no meaningful impact on vertical movement of the subsurface several feet below ground surface. As will be discussed later in the memo, there is substantial evidence that the shrinkage of clay soils caused the small amount of subsidence observed at the W2A Monitoring Segment.

Analysis of the Twentieth (20th) Re-measure of the Water Line W1A and W2A Monitoring Benchmark and Monitoring Point Elevations over a 1-year and a 11-year Period

W1A Segments

Tables 1 and 2 provide the differences in elevations for 18 monitoring benchmarks and 4 monitoring points located along the W1A Segment. The differences in the measured elevations for the last year and for the last 11 years are discussed below.

The discussion below excludes results from benchmark MbM-11. As discussed in previous analyses, the measured elevation change at benchmark MbM-11 is an outliner when compared to other measured differences in elevations along FM 2798. For instance, over an 11-year period, the elevation of benchmark MbM-11 decreased by 0.22 ft whereas benchmarks on both sides of MbM-11 averaged a decrease of 0.015 ft in elevation. The significantly higher amount of elevation change at MbM-11 is attributed to the benchmark being in a narrow zone of highly disturbed soil in the downthrown fault blocks. The higher rate of elevation change at MbM-11 is likely caused by the compaction of the highly disturbed soil.

Last year: Over the last year, the 18 monitoring benchmarks that comprise the Segment W1A Monitoring System along FM2978 had the following elevation changes:

- The four monitoring benchmarks on the upthrown side of the Egypt Fault ranged from no change in elevation to a decrease of 0.01 ft in elevation and averaged a decrease of 0.005 ft in elevation.

- After omitting results from benchmark MbM11, the thirteen monitoring benchmarks on the downthrown side of the Egypt Fault ranged from a decrease of 0.02 ft to 0.01 ft in elevation and averaged a decrease of 0.015 ft in elevation.

Over the last year, the four monitoring points that comprise the Egypt Fault Monitoring System along Research Forest Drive had the following elevation changes:

- The two monitoring points on the upthrown side of the Egypt Fault ranged from no change in elevation to a decrease of 0.01 ft in elevation and averaged a decrease of 0.005 ft in elevation.
- The two monitoring points on the downthrown side of the Egypt Fault had a decrease of 0.01 ft each in elevation.

From March 2025 to March 2026, our analysis of the elevation data from the W1A Segment indicates that the downthrown side of the fault has moved downward relative to the upthrown side of the fault.

Last 11 years: – From March 2015 to March 2026, the 18 monitoring benchmarks that comprise the Segment W1A Monitoring System along FM 2978 had the following elevation changes:

- The four monitoring benchmarks on the upthrown side of the Egypt Fault ranged from an increase of 0.01 ft in elevation to a decrease of 0.02 ft in elevation. The four monitoring benchmarks averaged 0.005 ft reduction in elevation.
- After omitting results from benchmark MbM-11, the thirteen monitoring benchmarks on the downthrown side of the Egypt Fault ranged from a decrease of 0.03 ft to 0.01 ft in elevation. The thirteen monitoring benchmarks averaged a change of a decrease of 0.02 ft in elevation.

From March 2015 to March 2026, the four monitoring points that comprise the Egypt Fault Monitoring System along Research Forest Drive had the following elevation changes:

- The two monitoring points on the upthrown side of the Egypt Fault had a decrease of 0.01 ft and 0.02 ft in elevation with an average decrease of 0.015 ft in elevation.
- The two monitoring points on the downthrown side of the Egypt Fault had a decrease of 0.06 ft and 0.070 ft in elevation with an average of 0.065 ft decrease in elevation.

During the last 11 years, the monitoring data indicates that more downward movement occurred on the downthrown side on the Egypt Fault. Along Research Forest Drive, the downthrown side of the fault averaged a decrease of 0.05 ft in elevation more than the upthrown side of the fault. This amount of elevation change indicates that the downthrown side of the Egypt Fault is subsiding at rate approximately 0.0045 ft/yr relative to the upthrown side of the Egypt Fault. Along FM 2978, the downthrown side of the fault averaged a decrease of 0.015 ft in elevation more than the upthrown side of the fault. These amounts of elevation change are too small to be consider conclusive evidence that land subsidence is occurring along Egypt Fault where it intersects FM 2978.

W2A Segments

Tables 3 and 4 provide the differences in elevations for 23 monitoring benchmarks and monitoring points located along the W2A Segment. The differences in measured elevations for the last year and for the last 11 years are discussed below.

Last year: – Over the last year, the four monitoring points that comprise the Big Barn Fault Monitoring System along Research Forest Drive in Figure 4 had the following elevation changes:

- The two monitoring points on the upthrown side of the Big Barn Fault had no change in elevation and an increase of 0.01 ft in elevation with an average change of 0.005 ft increase in elevation.
- The two monitoring points on the downthrown side of the Big Barn Fault had no change in elevation.

- Over the last year, the 19 monitoring benchmarks that straddle the suspected Panther Branch Fault along Research Forest Drive at the Segment W2A Monitoring System in Figure 5 had the following elevation changes:
  - The six monitoring benchmarks (MbM-13 through MbM-18) on the upthrown side of the suspected Panther Branch Fault had elevation changes that ranged from no change in elevation to a decrease of 0.01 ft in elevation.
  - The thirteen monitoring benchmarks (MbM-1 through MbM-12 and MbM-20) on the downthrown side of the suspected Panther Branch Fault had elevation changes that ranged from 0.01 ft to 0.02 ft decrease in elevation.

  From March 2025 to March 2026, the downthrown side of the suspected Panther Branch Fault along Research Forest Drive averaged 0.012 ft greater subsidence than the upthrown side of the suspected Panther Branch Fault.

Last 11 years: – From March 2015 to March 2026, the four monitoring points along Research Forest Drive near the Big Barn Fault in Figure 4 had the following elevation changes:

- The two monitoring points on the upthrown side of the Big Barn Fault ranged from no change in elevation to an increase of 0.01 ft in elevation and averaged an increase of 0.005 ft in elevation.
- The two monitoring points on the downthrown side of the Big Barn Fault ranged had a decrease of 0.03 ft in elevation.

The changes in the elevation of monitoring points that straddle the Big Barn Fault indicate that the downthrown side of the fault has subsided approximately 0.035 ft more than the upthrown side of the fault. A 0.035 ft decrease in relative elevation over 11 years translates into an average subsidence rate of approximately 0.0032 ft/yr

From March 2015 to March 2026, the 19 monitoring benchmarks located along Research Forest Drive near the suspected Panther Branch Fault in Figure 5 had the following elevation changes:

- The six monitoring benchmarks (MbM-13 through MbM-18) on the upthrown side of the suspected Panther Branch Fault ranged between no change in elevation to a decrease of 0.01 ft change in elevation and averaged a decrease of 0.007 ft in elevation.
- The thirteen monitoring benchmarks (MbM-1 through MbM-12 and MbM-20) on the downthrown side of the suspected Panther Branch Fault had elevation changes that ranged from a decrease of 0.06 ft to a decrease of 0.17 ft and averaged a decrease of 0.12 ft.

The changes in the elevation at the monitoring benchmarks near the suspected Panther Branch Fault indicate that the downthrown side of the fault has subsided approximately 0.11 ft more than the upthrown side of the fault. The 0.11 ft decrease in elevation over 11 years translates into an average subsidence rate of approximately 0.01 ft/yr since March 2015.

Figure 6 shows graphs for the average vertical displacement calculated for the benchmarks located on the upthrown side and the downthrown side of the suspected Panther Branch Fault as a function of time since March 2015. The graph shows that the downthrown side of the fault has consistently greater decrease in

elevation than the upthrown side. Whereas the upthrown side of the fault has not subsided more than 0.015 ft over a 1-year period within the 11-year monitoring period, the downthrown side of the fault has exhibited a general trend of declining elevation with greater displacement rates in the latter years. Over the 11-year monitoring period, the average net decline in elevation on the downthrown side of the Panther Branch Fault relative to the upthrown side was 0.0103 ft per year.

Figure 7 and **Table 5** show the rates of vertical displacement for the downthrown side of suspected Panther Branch Fault relative to the upthrown side of the suspected Panther Branch Fault. The relative rate is calculated by subtracting the rate of displacement of the upthrown side from the rate of displacement of the downthrown side. The temporal changes in the displacement have been divided into three periods: 1) from March 2015 to March 2019; 2) from March 2019 to March 2022; and 3) from March 2022 to March 2026.

Table 5 Vertical displacement rates for the downthrown side of Suspected Panther Branch Fault relative to the upthrown side of the Suspected Panther Branch Fault for Three Time Intervals

Time Period	Time Interval (years)	Average Vertical Displacement since 2015 (ft)	Incremental Amount of Vertical Displacement (ft)	Average Rate of Vertical Movement (ft/yr)
March 2015 to March 2019	4	-0.013	-0.013	-0.003
March 2019 to March 2022	3	-0.037	-0.024	-0.008
March 2022 to March 2026	4	-0.1134	-0.076	-0.019

Evaluation of Potential Damage to the Water Line along Segments W1A and W2A from Land Subsidence

To provide information beneficial to support a risk assessment of potential damage to the water line posed by land subsidence, INTERA compiled information on the design of these safeguards through construction drawings and discussions with persons knowledgeable of the safeguards. The construction drawings prepared by Lockwood, Andrews & Newnam, Inc. include the design of the casing pipe for the W1A area. The construction drawings by Binkley & Barfield Inc. include the design pipe for the W2A area. The design of the safeguards for the Big Barn Fault is based on the design used for where the Egypt Fault intersects the 48-inch water line.

W1A Segments

In the vicinity of the Egypt Fault Monitoring System along Research Forest Drive, SJRA's GRP 48-inch diameter water line is protected by a pipe casing along a 500-ft section that crosses over the Egypt Fault. The water line is constructed of steel and capable of shifting approximately 1-ft over the 500-ft interval. Because of the possibility that the water line could eventually have a differential movement of more than 1 ft, a pipe casing as a safeguard around the water line was constructed. The pipe casing safeguard is designed to protect the water line for up to 0.25 inches of vertical movement at the fault per year over a 50-year period. This amount of movement is equivalent to 12.5 inches over 50 years, which translates to an average rate of 0.021 ft/yr. The dip angle of the fault was estimated at 70 degrees. A 12.5-inch vertical movement is expected to cause the casing and pipe to bow and move horizontally up to 4 inches. The pipe and casing can deflect and "flex" with the vertical movement, but a horizontal movement of 4 inches could stress the steel enough to break the joints. To protect against the horizontal movement, two expansion couplings, each of which can move up to 4 inches horizontally, were added at the pipe connections. These

expansion joints allow up for 8 inches of horizontal movement. Several methods are in place to monitor the condition of the water line. One of these methods is measuring the change in elevations in the casing and pipe at the ends of the pipe casing.

After 11 years of monitoring the change in the monitoring point elevations at the Egypt Fault Monitoring System, the downthrown side of the fault had subsided 0.05 ft relative to the upthrown side of the fault. Thus, the average rate of subsidence of the downthrown side of the fault relative to the upthrown side of the fault is approximately 0.00455 ft/year. Based on the information that INTERA has reviewed, INTERA concludes the water line is not at risk of damage from land subsidence where it crosses the Egypt Fault along Research Forest Drive for the next 50 years if land subsidence continues at its current rate and if the SJRA safeguards work as designed.

Along FM 2978, the 16-inch water line extends to SJRA Woodlands Division Water Plant No. 4. Instead of using pipe casing to protect the water line, a SJRA contractor installed a series of ball connections in the vicinity of the Egypt Fault to accommodate movement of up to 0.25 inches of vertical movement per year over a 50-year period, or a total of 12.5 inches. Along a length of approximately 400 ft, six ball couplings were installed. During 11 years of monitoring, the average changes in the monitoring benchmark elevations are a decrease of 0.005 ft and 0.02 ft in elevation on the upthrown and downthrown side of the fault, respectively. Thus, the subsidence of the downthrown side of the fault relative to the upthrown side of the fault is approximately 0.015 over 11 years, which translates to 0.0014 ft/yr. Based on the information that INTERA has reviewed, INTERA concludes that the water line is not at risk of damage from land subsidence where it crosses the Egypt Fault along FM 2978 for the next 50 years if land subsidence continues at its current rate and if the SJRA safeguards work as designed.

W2A Segments

INTERA has reviewed the drawings for the safeguards that SJRA's contractor constructed for the transmission pipe at the Big Barn Fault Monitoring System. The safeguards are similar to the safeguards SJRA's contractor constructed using pipe casing for the Egypt Fault. The average change in the monitoring benchmark elevations at the Big Barn Fault over 11 years for the upthrown side and for the downthrown side of the Big Barn Fault are an increase of 0.005 ft and a decrease of 0.030 ft in elevation, respectively. Thus, the decrease of the downthrown side of the fault relative to the upthrown side is 0.035 ft over 11 years, or approximately 0.0032 ft/yr. The safeguards that were constructed are designed to handle 12.5 inches of vertical movement over 50 years or approximately 0.021 ft/year. Based on the information that INTERA has reviewed, INTERA concludes that the water line is not at risk of damage from land subsidence where it crosses the Big Barn Fault along Research Forest Drive for the next 50 years if land subsidence continues at its current rate and if the SJRA safeguards work as designed.

Because the Fugro report (2012) did not show that the suspected Panther Branch Fault crossing the water line, SJRA's consultant did not design nor did SJRA's contractor construct safeguards to protect the water line from differential subsidence associated with the suspected Panther Branch Fault. The average change in the monitoring benchmark elevations at the suspected Panther Branch Fault over 11 years for the upthrown side and for the downthrown side of the suspected Panther Fault are a decrease of 0.007 ft and a decrease of 0.12 ft in elevation, respectively. Thus, the decrease of the downthrown side of the fault relative to the upthrown side is about 0.113 ft over 11 years, or approximately 0.0103 ft/yr. Figure 7 shows that since March 2022, the elevation decreased by an average rate of 0.019 ft/yr. Per discussion with SJRA, SJRA plans to continue to monitor subsidence using the benchmarks associated with the Segment W2A Monitoring System and to investigate what safeguards may be needed to protect the transmission line.

Investigation into Temporal Variability in the Measured Elevation Change along the Suspected Panther Branch Fault

Figures 6 and 7 show a cyclic pattern in the vertical displacement that is characterized by greater subsidence occurring during the summer months than winter months. Figure 8 and Table 6 show the vertical displacements that have occurred during the 6-month interval preceding the March and September measured benchmark elevations from 2015 to 2024. For the 6-month interval from March to September, subsidence occurs on both sides of the fault, whereas for 6-month interval from September to March, rebound occurs on both sides of the fault. For both six-month intervals, the vertical offsets are much greater for the downthrown benchmarks than for the upthrown benchmarks. For both sets of benchmarks, the magnitude of the vertical displacements has steadily increased over time with the greatest rate of increases having occurred during the latter years.

Table 6 Vertical displacement that occurred during the 6-month intervals preceding the March and September measurements of elevations at the benchmarks associated with the Segment W2A Monitoring System along the suspected Panther Branch Fault.

Date (Month/Yr)	Vertical Displacement (feet)		Date (Month/Yr)	Vertical Displacement (feet)	
	Downthrown Side	Upthrown Side		Downthrown Side	Upthrown Side
Sep-15	-0.0108	-0.0050	**Mar-16**	0.0008	0.0050
Sep-16	0.0000	-0.0033	**Mar-17**	0.0015	0.0033
Sep-17	-0.0054	0.0000	**Mar-18**	0.0015	0.0000
Sep-18	-0.0077	-0.0050	**Mar-19**	0.0069	0.0050
Sep-19	-0.0131	-0.0050	**Mar-20**	0.0023	0.0017
Nov-20	-0.0108	-0.0033	**Mar-21**	0.0015	0.0050
Sep-21	-0.0046	-0.0017	**Mar-22**	0.0008	0.0033
Sep-22	-0.0354	-0.0100	**Mar-23**	0.0062	0.0067
Sep-23	-0.0385	-0.0100	**Mar-24**	0.0062	0.0067
TOTAL	*-0.1262*	*-0.0433*	***TOTAL***	*0.0277*	*0.0367*

The cyclic pattern in the vertical displacement is consistent with presence of expansive soils (Barthélémy and others, 2023; Charpentier and others, 2022; Kai and others., 2020; Mostafiz and others, 2021; Wang, 2022). Expansive soils contain clays that can undergo volume change in response to fluctuations in soil moisture. During periods of high moisture content, these soils swell, expanding their volume. During periods of low-moisture content, expansive soils dry, which causes a reduction in their volume. The cyclic pattern of vertical displacement occurs because of seasonal changes in evapotranspiration (ET). In the Gulf Coast of Texas, ET is lowest from November through February (~20% of annual total over five months) and highest in other months with maximum monthly totals occurring between June and August for different locations (Scanlon and others, 2012).

As a general rule, the shrinkage that occurs as a result of the drying of soils is considered elastic. Elastic deformation means the full amount of shrinkage is fully recoverable under the right set of circumstances. In the case of shrinkage caused by desiccation, rewetting of the soil would cause the soil to expand back to its original volume. However, in a recent study of expansive soils in Harris County, Welch and others (2024) discovered that a fraction of the shrinkage that occurs during drying is inelastic deformation. Inelastic deformation refers to the permanent change in the volume or shape of the soil that does not revert under rewetting. Welch and others (2024) conclude that during periods of prolonged drought, approximately 10% of their total subsidence that occurs because of shrinkage of expansive soils is inelastic. Notably, this effect of inelastic subsidence results in a step-like permanent loss of land elevation over time.

A primary factor that contributes to seasonal patterns of drying and wetting of soils is evapotranspiration (ET). Figure 9 shows monthly values for evapotranspiration at the Segment W2A Monitoring System obtained from the OpenET data portal (https://etdata.org). The OpenET values presented here are an ensemble average of six different algorithms based on thermal satellite data and auxiliary data (Melton and others, 2022). The monthly values show a distinctive cyclic pattern with approximately 270% greater ET from March to September than from September to March. Besides ET, the monthly Palmer Drought Severity Index (PDSI) values in Figure 10 are consistent with the cyclic pattern in the vertical displacement and the greatest subsidence rates during the summer of 2022 and 2023. PDSI data for Montgomery County was obtained from the Western Regional Climate Center (2024).

The PDSI is used to estimate the relative dryness of the soil and is calculated from ET, rainfall, the soil water holding capacity from soil map developed by the National Cooperative Soil Survey. PSDI values range from +10 to -10 with lower number represent drier conditions. Table 7 provides additional details on the soil's classifications associated with the PSDI numbers. Among the saline features in Figure 10 are:

- Before January 2020, the PDSI was primarily greater than 3 indicating very wet to extremely wet soil conditions for both summer and winter months which is consistent with the smaller amounts of vertical displacements from 2015 to 2019 in Figure 8;
- From January 2021 to June 2023, the PDSI was less than 2 and average about 0 indicating drier moisture conditions than the conditions for the previous 6 years, which is consistent with increasing in the rate of vertical displacements in Figure 8;
- During summer months from 2021 to 2023 where moderate drought conditions existed, Figure 8 shows that the largest amounts of subsidence occurred. Based on the correlations observed between PDSI and changes in land elevation (which are discussed later in the report) the shrinkage of clayey soil is the most likely cause for the observed subsidence.
- From Fall 2023 to December 2024, the PDSI values greater than 3 indicate very wet to extremely wet soil conditions. During a portion of that time interval, Figure 7 shows that the rate of subsidence was similar to the low rate that occur prior to January 2020 when wet soil conditions also prevailed. The occurrence of low subsidence rate and rebounds during periods with high PDSI values is presented later in the report support the conclusions that the shrinkage of clayed soil is the most likely cause for the observed subsidence at the W2A Segment.

Besides causing the expansive soils to subside, drought conditions can indirectly affect land subsidence by impacting the amount of water used by homeowners. As a general rule, homeowners will water their lawn more during drought conditions than during wet conditions unless regulated not to do so. Consequently, water use tends to peak during the summer months as is reflected in monthly pumping amounts shown in Figure 11. Figure 11 shows SJRA pumping from the Evangeline and the Jasper aquifers.

Among the potentially important features of Figure 11 is the increases in the production from the Evangeline aquifers in 2022 and 2023. If this increase in production caused a reduction in the water pressure, then the higher pumping rates would have contributed to the increase in the subsidence rates during the summer months in 2022 and 2023.

Based on our analysis, subsidence typically occurs during the summer months and rebound typically occurs during the winter months. Two factors that contribute to this cyclic pattern between rebound and subsidence are related to seasonal changes in the weather. One factor is the wetting and drying of expansive soils during the winter months and summer months, respectively. The other factor is that pumping is typically higher in the summer months. During the periods of increased pumping, the hydrostatic pressure in the saturated aquifer is reduced, which in turn may cause consolidation of the aquifer matrix.

Table 7 PDSI values classification of Soil Conditions

PDSI value	Soil Classification
4.0 or more	extremely wet
3.0 to 3.99	very wet
2.0 to 2.99	moderate wet
1.0 to 1.99	slightly wet
0.5 to 0.99	incipient wet spell
0.49 to -0.49	near normal
-0.5 to -0.99	incipient dry spell
-1.0 to -1.99	mild drought
-2.0 to -2.99	moderate drought
-3.0 to -3.99	severe drought
-4.0 or less	extremely drought

Before proceeding with additional discussion of the measured benchmarks, there are two issues that merit discussion. One issue is that the benchmarks measure elevation changes occur at a shallower depth than 10 feet, which is the approximate depth of the SJRA transmission line. Soil movement caused by moisture changes is expected to be smaller at 10 feet depth because evaporation mainly affects shallow soils near the surface. The other issue is that the benchmarks are located approximately 100 feet away from the SJRA transmission line on the other side of Research Forest Drive. Thus, our analysis does not account for any differences that may exist between the soil and fault between the two locations that would impact land subsidence.

The amount that each of these factors contributed to subsidence cannot be estimated without additional information. Among the data that would be needed to help provide these estimates is the amount and nature of the expansive soils that exist near the benchmarks and the changes of hydraulic pressure that occur in the aquifer as a result of changes in pumping rates.

References

Barthélémy, S., Bonan, B., Calvet, J.-C., Grandjean, G., Mon Coulon, D., Kapsambelis, D., & Bernardie, S. 2023. A new drought index fitted to clay shrinkage induced subsidence over France: Benefits of interactive leaf area index. EGUsphere. https://doi.org/10.5194/egusphere-2023-1366

Charpentier, A., James, M., & Ali, H. 2022. Predicting drought and subsidence risks in France. Natural Hazards and Earth System Sciences, 22(7), 2401–2418. https://doi.org/10.5194/nhess-22-2401-2022

Fugro Consultants, Inc., 2012. Geologic Fault Delineation Study SJRA Distribution Lines – Route W1 San Jacinto River Authority Montgomery County, Texas. Report No. 04.12110014-9 Prepared for Lockwood, Andrews & Newnam, Inc., Houston Texas.

Kai, L., Liang, K., Hossein, N., & Cyrille, C. 2020. The mechanical behavior of an expansive soil due to long-term seasonal rainfalls. E3S Web of Conferences, 195, 02019.https://doi.org/10.1051/e3sconf/202019502019

Melton, F.S., Huntington, J., Grimm, R., Herring, J., Hall, M., Rollison, D., Erickson, T., Allen, R., Anderson, M., Fisher, J.B. and Kilic, A., 2022. OpenET: Filling a critical data gap in water management for the western United States. JAWRA Journal of the American Water Resources Association, 58(6), pp.971-994.

Mostafiz, R. B., Friedland, C. J., Rohli, R. V., Bushra, N., & Held, C. L. 2021. Property risk assessment for expansive soils in Louisiana. Frontiers in Built Environment, 7, 1–10. https://doi.org/10.3389/fbuil.2021.754761

Scanlon, B.R., R. Reedy, G. Strassberg, Y. Huang, and Y.G. Senay. 2012. Estimation of Groundwater Recharge to the Gulf Coast Aquifer System in Texas, USA. Unnumbered Report: Texas Water Development Board.

Wang, G. (2012). Kinematics of the Cerca del Cielo, Puerto Rico landslide derived from GPS observations. Landslides, 9(1), 117–130. https://doi.org/10.1007/s10346-011-0277-5

Welch, J., Wang, G., Bao Y., Zhang, S., Huang, S., and H. Xie. 2024. Unveiling the Hidden Threat: Drought-Induced Inelastic Subsidence in Expansive Soils. Geophysical Research Letters, Vol. 51. Issue 7. https://doi.org/10.1029/2023GL107549

Western Regional Climate Center. 2024. West Wide Drought Tracker. Retrieved from https://wrcc.dri.edu/wwdt/

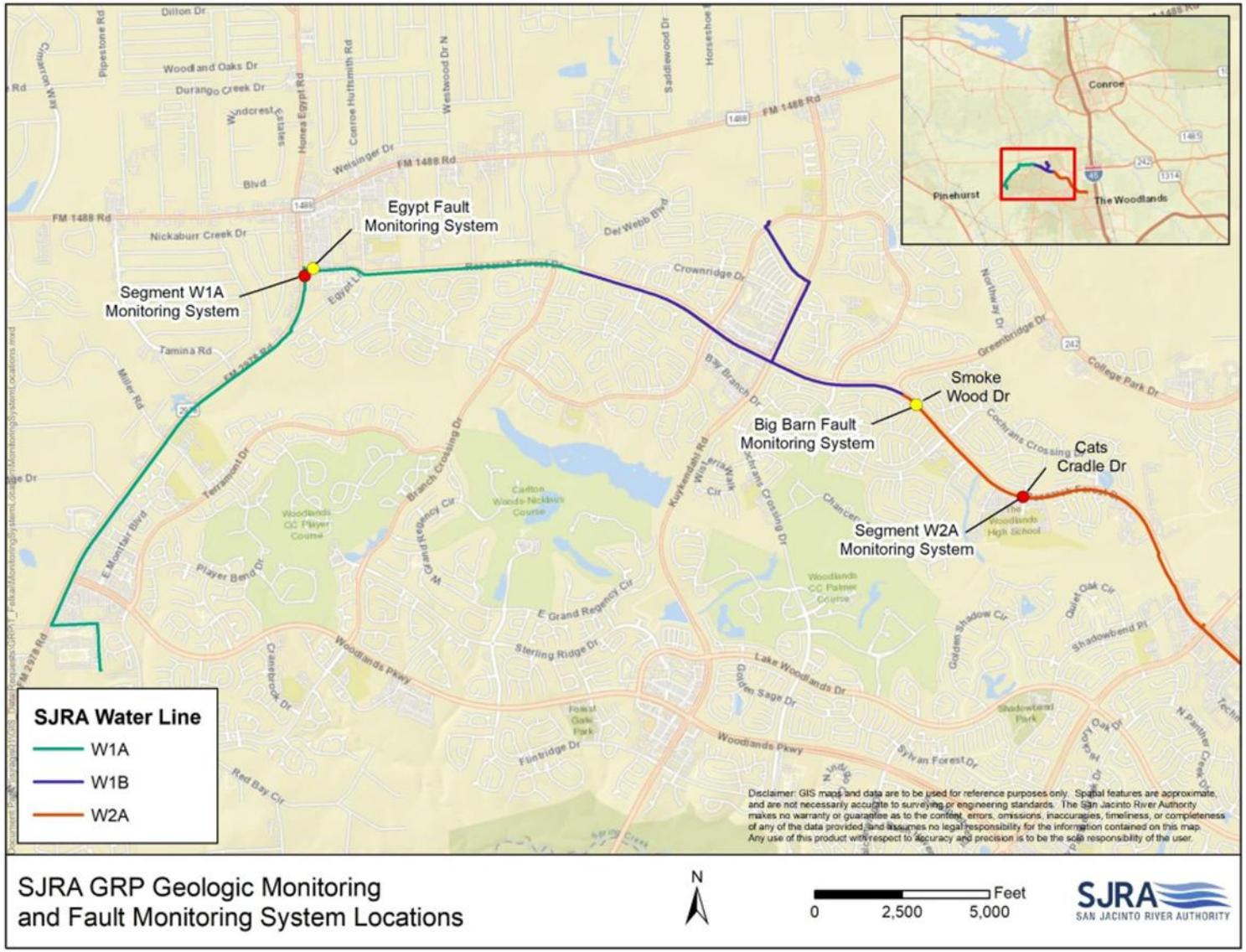

Figure 1 SJRA Groundwater Reduction Plan (GRP) Fault Monitoring System Locations (https://www.sjra.net/grp/fault-monitoring/)

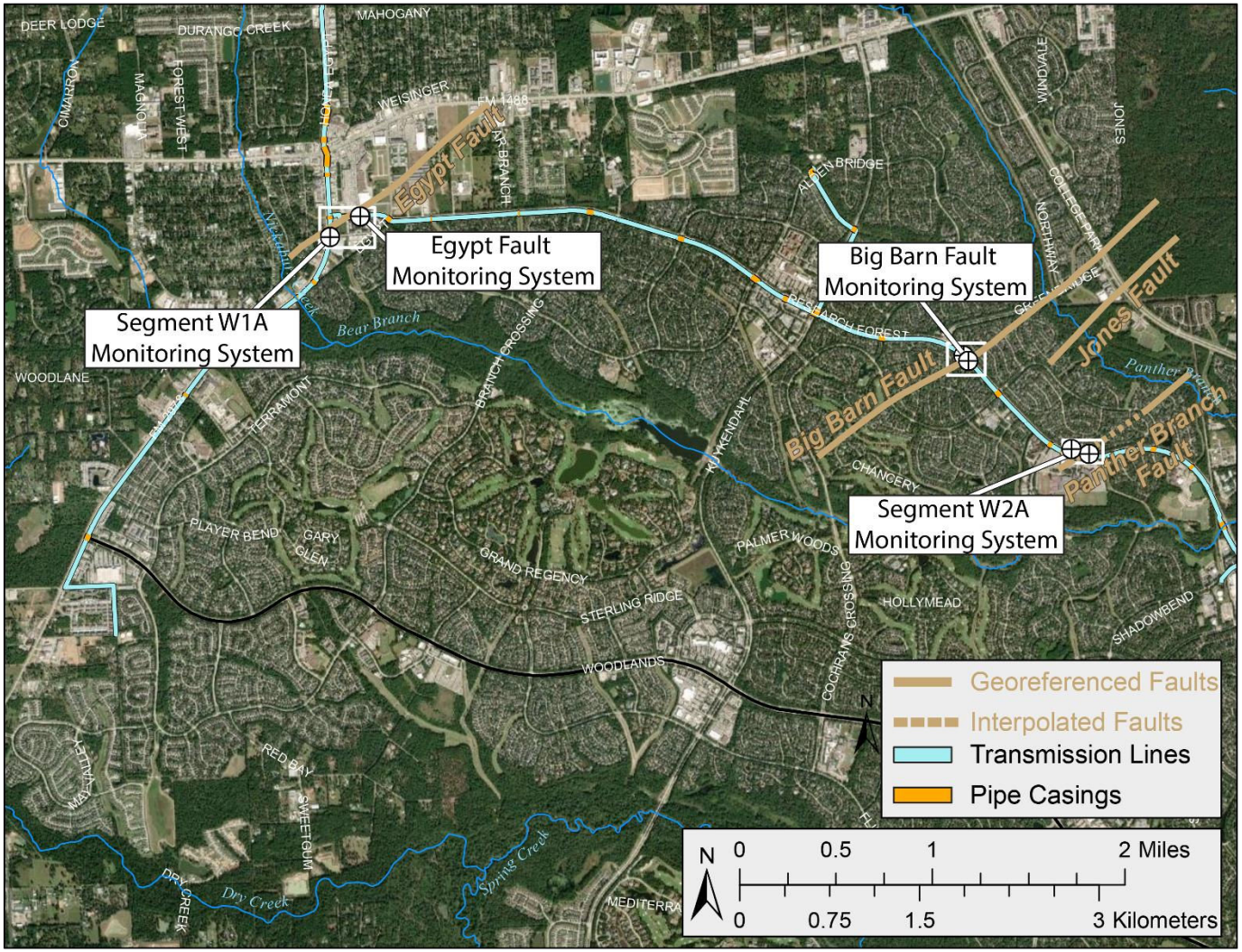

Figure 2 Satellite map showing the location of the SJRA water line, the fault locations mapped by Fugro (2012), and SJRA monitoring systems.

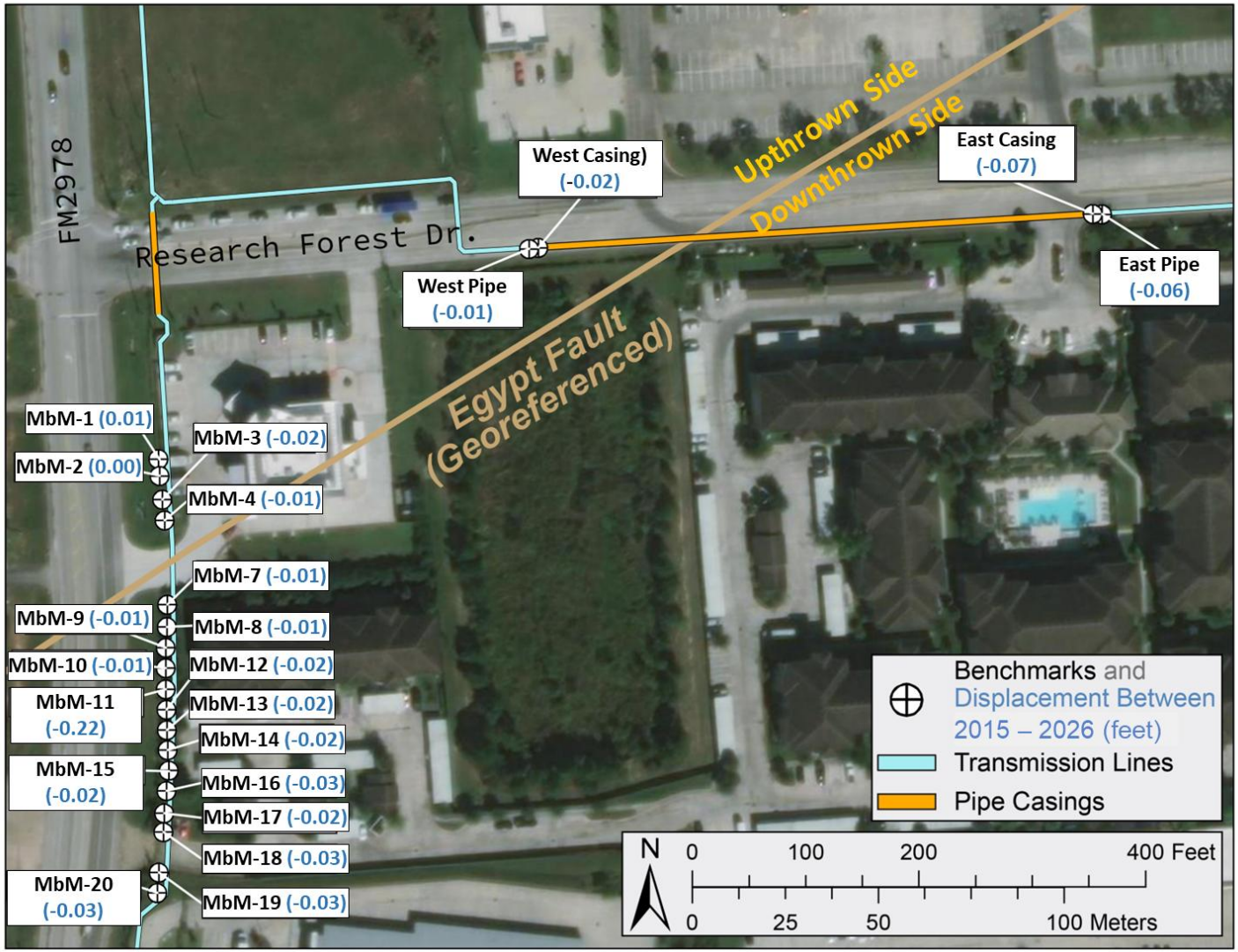

Figure 3 Satellite map showing the location of the Egypt Fault (Fugro, 2012), the W1A monitoring locations and calculated vertical displacement from March 2015 to March 2026 and the SJRA water line and pipe casing.

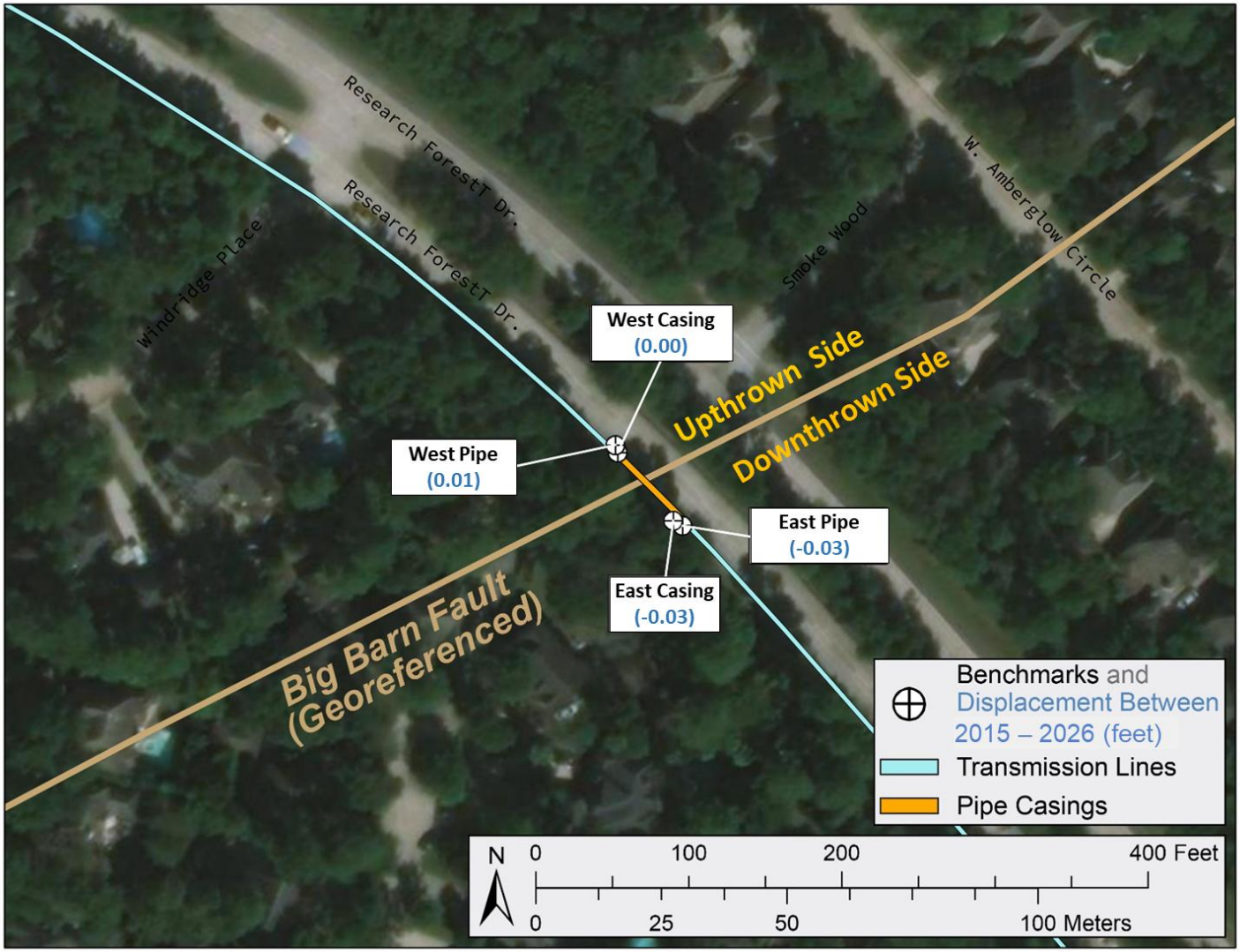

Figure 4 Satellite map showing the location of the Big Barn Fault (Fugro, 2012), the Big Barn Fault Monitoring System, calculated vertical displacement from March 2015 to March 2026, and the SJRA water line and pipe casing.

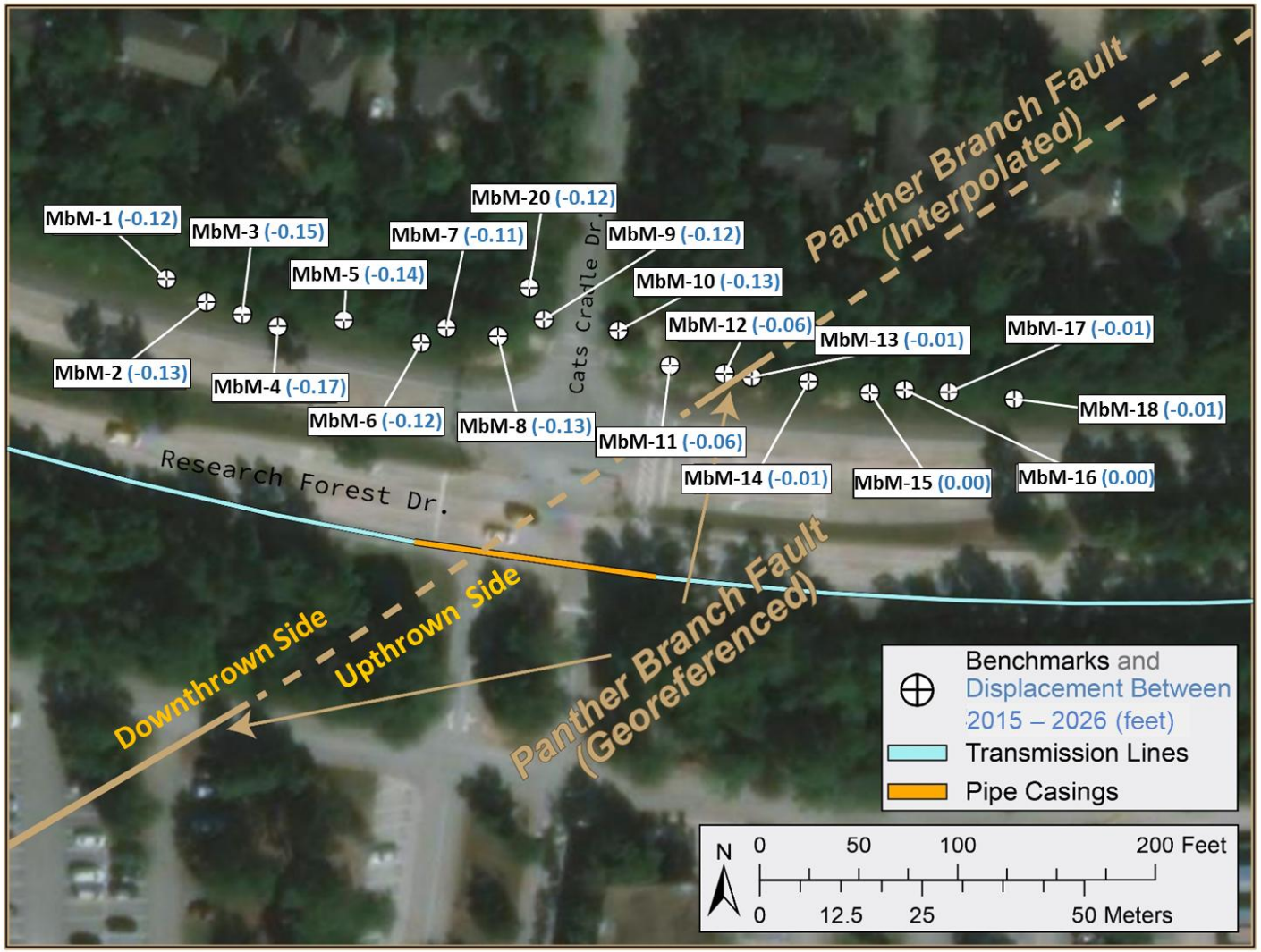

Figure 5 Satellite map showing the location of the suspected Panther Branch Fault mapped by INTERA, the Segment W2A Monitoring System, calculated vertical displacement from March 2015 to March 2026, and the SJRA water line and pipe casing.

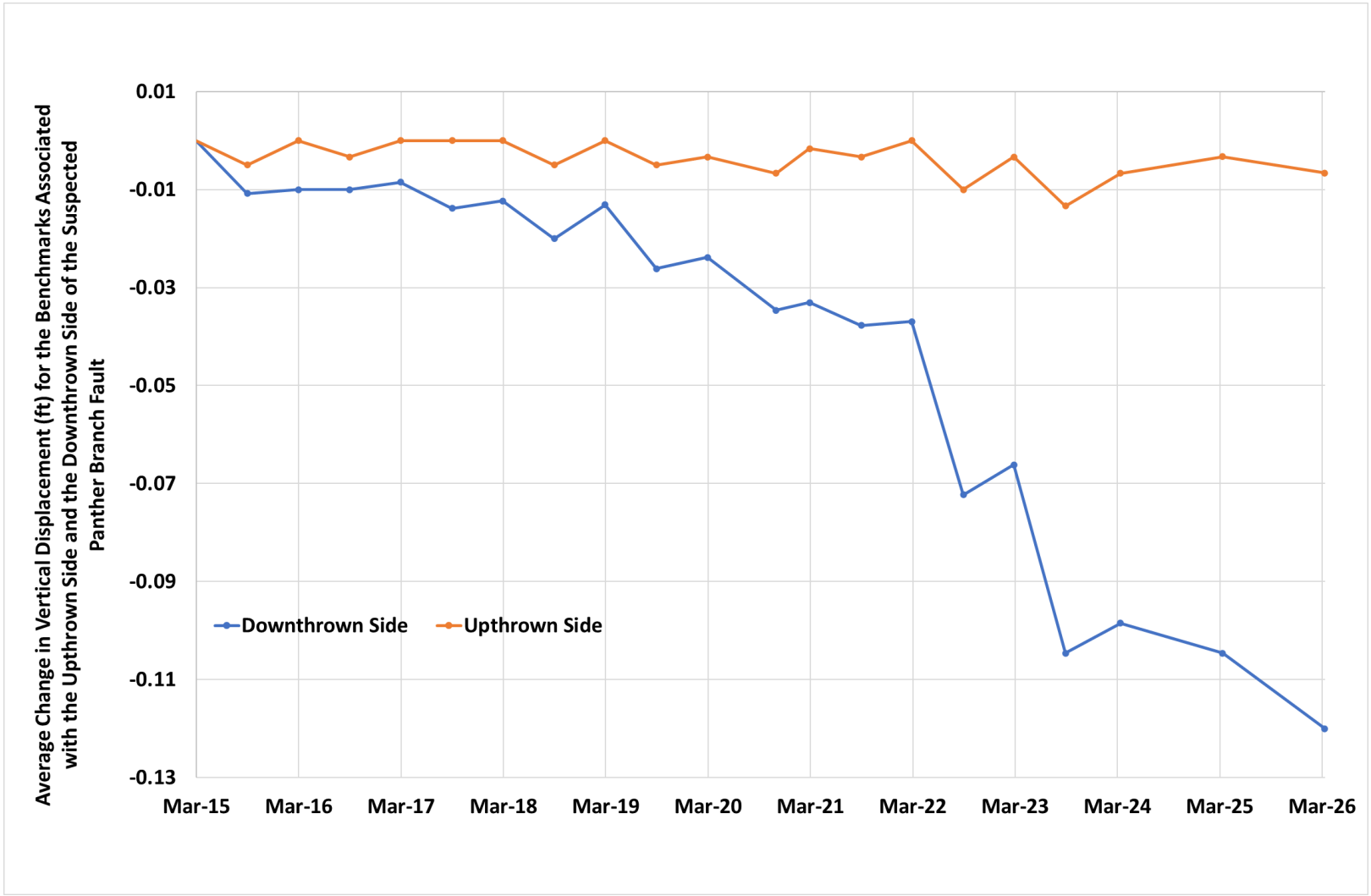

Figure 6 Comparison of average vertical displacement for the benchmarks located on the upthrown side and the downthrown side of the suspected Panther Branch Fault associated with the Segment W2A Monitoring System.

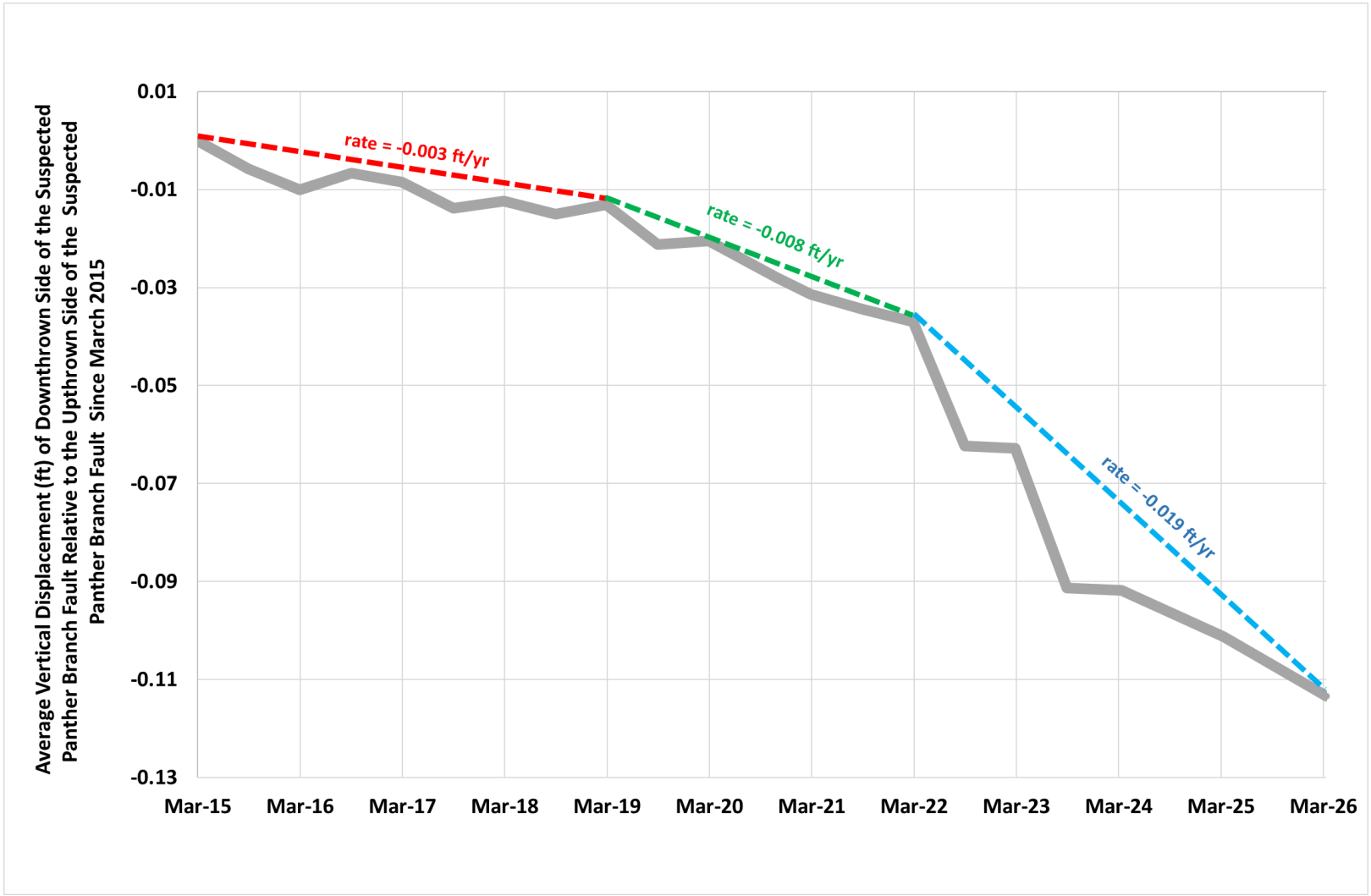

Figure 7 Relative vertical displacement and rates for relative vertical displacement for the downthrown side of the suspected Panther Branch Fault based on benchmarks associated with the Segment W2A Monitoring System

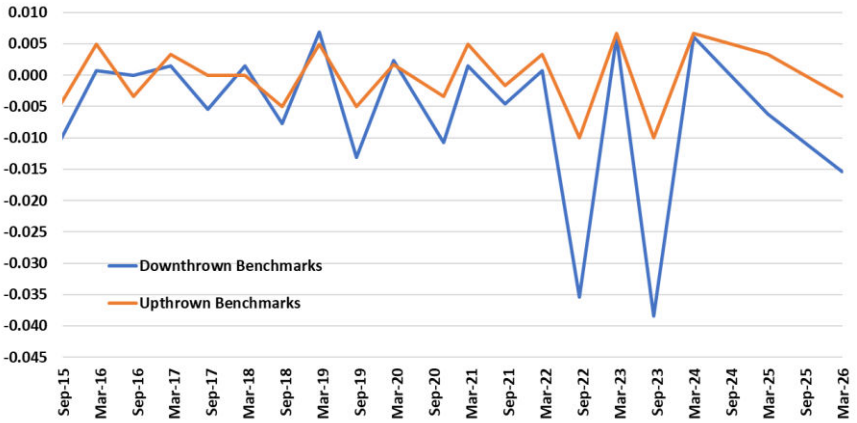

Figure 8 Vertical displacement that occurred during 6-months to 1-year intervals preceding the March and September measurements of benchmark elevations associated with Segment W2A Monitoring System along the suspected Panther Branch Fault.

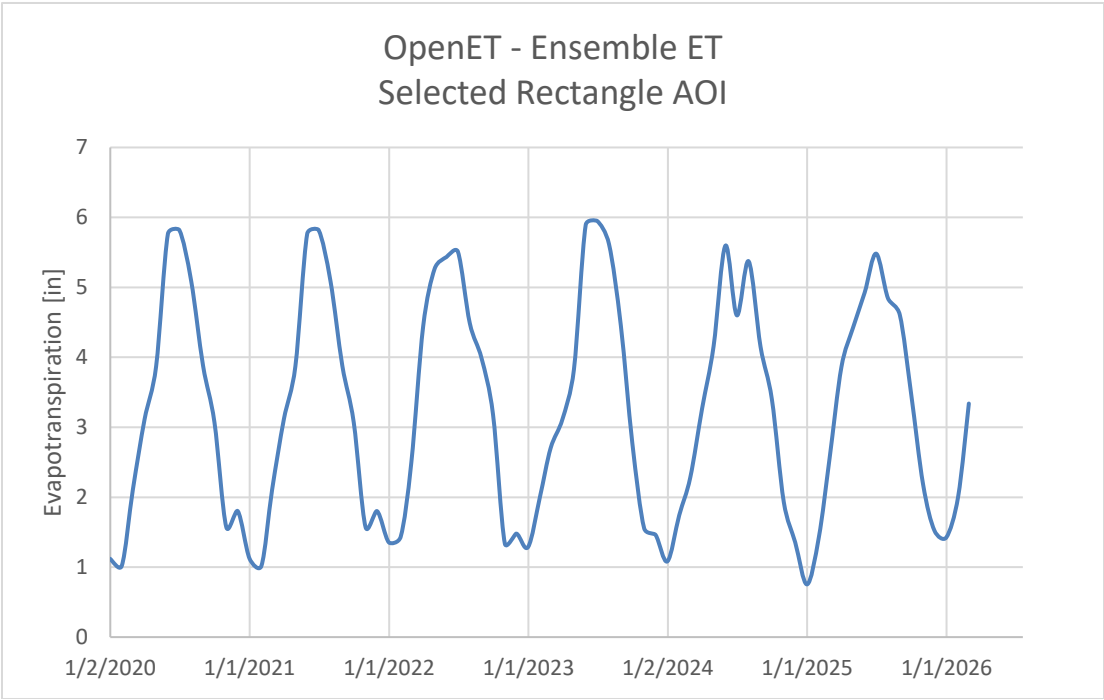

Figure 9 Monthly evapotranspiration (ET) amounts obtained for Segment W2A Monitoring System along the suspected Panther Branch Fault by OpenET (https://etdata.org/faq). Average cumulative ET amount from March to September and from September to March is about 25 inches and about 10 inches, respectively.

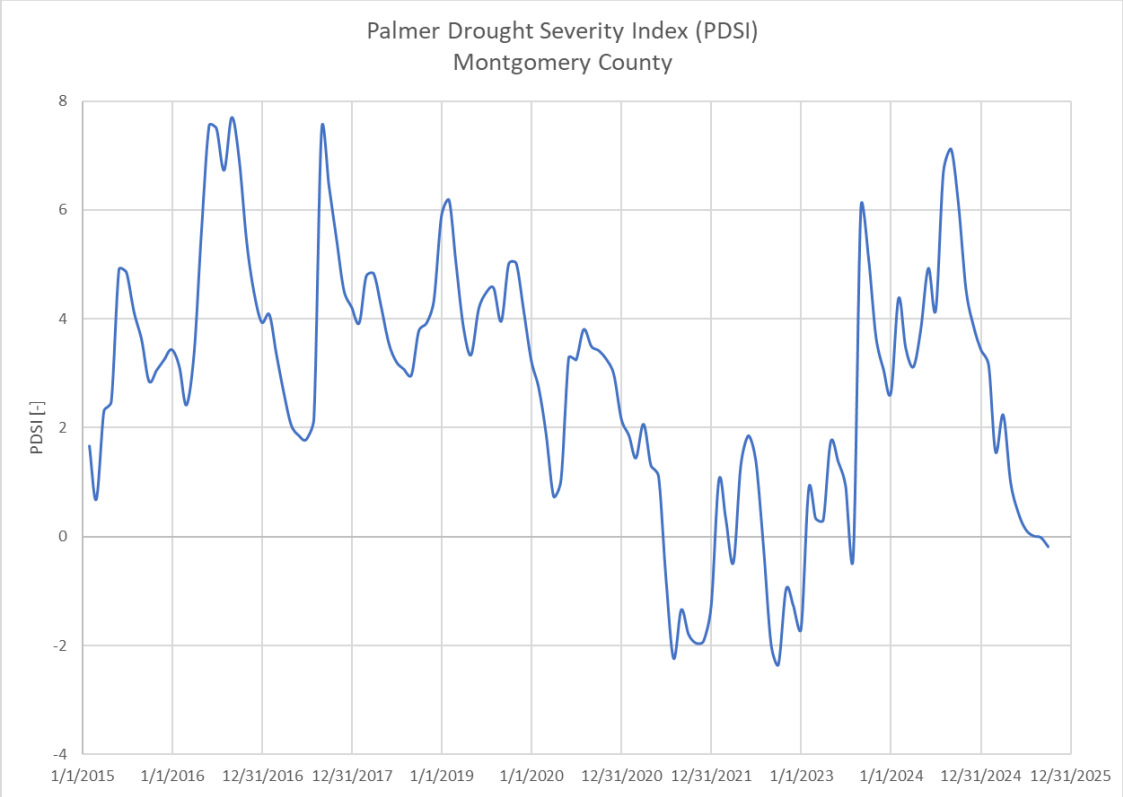

Figure 10 Monthly values for the Palmer Drought Severity Index (PSDI) form estimating relative dryness of soils for Montgomery County (from https://wrcc.dri.edu/wwdt/time/.)

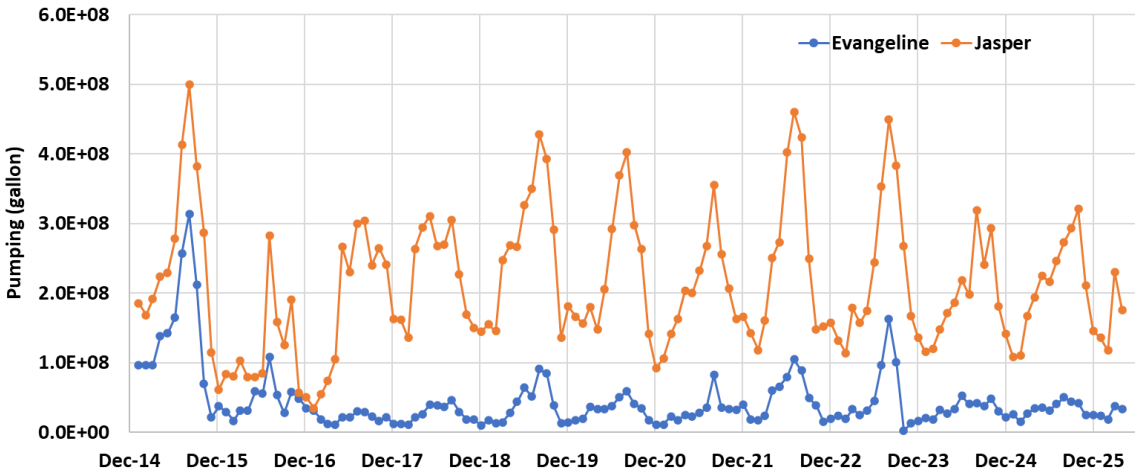

Figure 11 Monthly production from the Woodlands Wells from the Evangeline and Jasper aquifers.